Eur J Nucl Med Mol Imaging (2011) 38:23–36
DOI 10.1007/s00259-010-1588-9

ORIGINAL ARTICLE

Positron emission mammography in breast cancer presurgical planning: comparisons with magnetic resonance imaging

Kathy Schilling · Deepa Narayanan · Judith E. Kalinyak · Juliette The · Maria Victoria Velasquez · Simone Kahn · Matthew Saady · Ravinder Mahal · Larraine Chrystal

Received: 11 June 2010 / Accepted: 29 July 2010 / Published online: 25 September 2010

Abstract
Purpose The objective of this study was to compare the performance characteristics of ^{18}F-fluorodeoxyglucose (FDG) positron emission mammography (PEM) with breast magnetic resonance imaging (MRI) as a presurgical imaging and planning option for index and ipsilateral lesions in patients with newly diagnosed, biopsy-proven breast cancer.
Methods Two hundred and eight women >25 years of age (median age=59.7±14.1 years) with biopsy-proven primary breast cancer enrolled in this prospective, single-site study. MRI, PEM, and whole-body positron emission tomography (WBPET) were conducted on each patient within 7 business days. PEM and WBPET images were acquired on the same day after intravenous administration of 370 MBq of FDG (median=432.9 MBq). PEM and MRI images were blindly evaluated, compared with final surgical histopathology, and the sensitivity determined. Substudy analysis compared the sensitivity of PEM versus MRI in patients with different menopausal status, breast density, and use of hormone replacement therapy (HRT) as well as determination of performance characteristics for additional ipsilateral lesion detection.
Results Two hundred and eight patients enrolled in the study of which 87% (182/208) were analyzable. Of these analyzable patients, 26.4% (48/182), 7.1% (13/182), and 64.2% (120/182) were pre-, peri-, and postmenopausal, respectively, and 48.4% (88/182) had extremely or heterogeneously dense breast tissue, while 33.5% (61/182) had a history of HRT use. Ninety-two percent (167/182) underwent core biopsy for index lesion diagnosis. Invasive cancer was found in 77.5% (141/182), while ductal carcinoma in situ (DCIS) and/or Paget's disease were found in 22.5% (41/182) of patients. Both PEM and MRI had index lesion depiction sensitivity of 92.8% and both were significantly better than WBPET (67.9%, $p<0.001$, McNemar's test). For index lesions, PEM and MRI had equivalent sensitivity of various tumors, categorized by tumor stage as well as similar invasive tumor size predictions with Spearman's correlation coefficient of 0.61 for both PEM and MRI compared to surgical pathology. Menopausal status, breast density, and HRT did not influence the sensitivity of PEM or MRI. For 67 additional unsuspected ipsilateral lesions or multifocal lesions, PEM had sensitivity of 85% (34/40) and specificity of 74%, (20/27) compared to MRI's sensitivity of 98% (39/40) and specificity of 48% (13/27) [$p=0.074$, for sensitivity; $p=0.096$ for specificity]
Conclusion PEM is a good alternative to MRI as a presurgical breast imaging option and its performance characteristics are not affected by patient menopausal/hormonal status or breast density.

Keywords Breast · Cancer · Presurgical · PEM · WBPET · MRI

K. Schilling (✉) · J. The · M. V. Velasquez · S. Kahn · M. Saady · R. Mahal · L. Chrystal
Radiology Department, Boca Raton Regional Hospital,
800 Meadows Road,
Boca Raton, FL 33486, USA
e-mail: KSchilling@brch.com

D. Narayanan · J. E. Kalinyak
Naviscan, Inc.,
San Diego, CA 92121, USA

Present Address:
D. Narayanan
National Cancer Institute,
Bethesda, MD 20892-2580, USA

Introduction

The unifying premise in breast cancer screening is that early diagnosis can result in decreased patient morbidity and mortality. Breast cancer has seen this type of reduction since the implementation and attendance of mammographic screening programs [1, 2]. While mammography and ultrasound along with physical breast examination saves lives, it is not perfect since 10–15% of cancers are missed due to a variety of reasons including observer error, often because the cancer is hidden by dense normal parenchymal tissue [3, 4]. Once cancer is identified, an important diagnostic necessity is the accurate determination of the full extent of disease, as this directly impacts the type of surgical intervention and postoperative therapy the patient receives. Ultrasound, whole-body positron emission tomography (WBPET), and magnetic resonance imaging (MRI) are adjunct diagnostic modalities that have been employed to assist in determining the stage and extent of breast cancer prior to surgery. However, breast imaging is responsible for approximately 1 million surgical and needle breast biopsies being performed each year for benign findings [5]. In addition, second and third operations occur because of positive surgical margins on lumpectomy or partial mastectomy specimens in 40–60% of breast cancer patients [5]. These data highlight the need for improvement in distinguishing benign from malignant disease and accurately determining the extent of disease.

The use of dynamic contrast-enhanced MRI of the breast for presurgical planning had an enthusiastic start in the early 1990s. MRI has been successfully implemented in many medical communities as a valuable tool to diagnose additional cancer in the same breast (ipsilateral) in up to one third of patients and is recommended as a supplemental screening tool to mammography in women considered to be at high risk for developing breast cancer [6]. A clear advantage of MRI is that it does not use radioactivity and detects blood flow to lesions. Also, MRI is more sensitive and accurate than mammography and ultrasound in detection of invasive lobular cancer (ILC), which occurs at a higher rate in women with a history of hormone replacement therapy (HRT) [7]. MRI is sometimes referred to as molecular imaging because the patient is scanned before and after the intravascular injection of a contrast agent [8, 9]. Pre-contrast images are "subtracted" from the post-contrast images, and the kinetics of blood flow to particular lesions plotted. The increased blood flow is indicative of vascularization frequently found in cancer. However, the unprecedented sensitivity of MRI in identifying anatomical lesions and many benign lesions [10], its lower sensitivity for detection of in situ cancers [9], lack of uniform MRI-biopsy capability [11] and the lack of adherence to guidelines regarding image acquisition and interpretation hinders its use [12]. Challenges also arise with MRI interpretation when the breast is under estrogen modulation (menstrual cycle, HRT) which affects the glandular tissue of the breast, thus increasing image background [13]. For many women, the exam is a challenge for other reasons including claustrophobia, large body size, and implanted metal devices [14]. Further difficulty arises for those with impaired renal function for whom the intravenous contrast is contraindicated [15, 16].

Molecular imaging, using PET, has evolved over the past decade to become an integral step in the evaluation of patients with many different types of malignancies [17–19]. An advantage of PET is the use of radiotracers that can potentially detect cancer even prior to vascularization as cancer cell metabolism is usually heightened prior to the stimulation of new vessel growth. However, the use of WBPET in breast cancer is restricted in part due to the lower levels of ^{18}F-fluorodeoxyglucose (FDG) tracer uptake in some breast malignancies compared to other cancers and the small size of many screen-detected malignancies [20]. Detection of ILC and ductal carcinoma in situ (DCIS) with WBPET has been particularly challenging [20]. High-resolution breast PET, also known as positron emission mammography (PEM), is a small, organ-specific PET device with a reported in-plane spatial resolution of 2 mm. In addition, it has the unique capability of providing PET biopsy guidance that facilitates percutaneous sampling of identified lesions [17, 19]. A published multicenter, retrospective clinical study of 94 patients with equivocal or suspicious mammograms demonstrated that PEM has a sensitivity of 90%, specificity of 86%, and accuracy of 88% [21].

The main objective of this study was to prospectively compare the sensitivity of PEM versus breast MRI in depiction of known malignancies (index lesions) and to determine the performance characteristics of the two modalities for additional ipsilateral lesion detection in patients with newly diagnosed, biopsy-proven breast cancer as part of their presurgical planning. The sensitivity of PEM was compared with WBPET imaging on the same radiotracer dose administered to the same patients. Substudy analysis compared the sensitivity of PEM versus MRI with regards to menopausal status, breast density, and HRT use.

Materials and methods

Patient population

All persons gave their informed written consent prior to study inclusion. This single-site, prospective, Institutional Review Board-approved study (Boca Raton Regional Hospital) was designed and funded by the Radiology

Department at Boca Raton Regional Hospital (Boca Raton, FL, USA) to test the role of PEM and MRI in presurgical management of patients with newly identified, histopathologically characterized breast cancer lesions.

Women who were >25 years (median age=59.7± 14.1 years, range 29–87) were approached for participation from 1 September 2006 to 1 August 2008. In addition to patient age, clinical findings, and family history, medications and the presence of coexisting medical conditions were recorded.

All women had biopsy-proven primary breast cancer and were required to have a mammogram within 3 months prior to enrollment and were not participating in a similar, competing protocol [22]. The average time period between the diagnostic biopsy and imaging was 11.9 days. PEM, MRI, and WBPET imaging were conducted on each patient within 7 business days. The order of PEM and MRI imaging was dependent on device availability as is typical in routine clinical practice. To minimize radiation to the patient, the protocol allowed patients to be imaged by PEM followed by WBPET on the same dose of radiotracer. The patient's family history and medications were recorded and those who were pregnant, lactating, had type 1 or uncontrolled type 2 diabetes mellitus, or scheduled for a sentinel node procedure within 6 h of the PEM study were excluded. Those patients who had any tissue sampling intervention between PEM or MRI imaging, or underwent neoadjuvant chemotherapy or hormone therapy prior to definitive surgery, were excluded from analysis. For purposes of this scientific communication, we will focus on the data generated for index and additional ipsilateral lesion characterization by PEM and MRI.

MRI image acquisition

A 1.5-T Symphony whole-body system (Siemens Medical Solutions, Malvern, PA, USA), a 7-channel breast array coil, and an IV angiocatheter (minimum 20-gauge) in an antecubital fossa vein connected to a power injector were used. The imaging protocol consisted of an initial rapid gradient-echo scout localization sequence acquired in all three orthogonal planes. Non-contrast sequences included a turbo short τ inversion recovery (STIR) coronal sequence to image the breast, T spine, and axillary regions [30 sections; each section 4 mm and skip 1 mm; 340-mm field of view; repetition time (TR)/echo time (TE) 4030/30; inversion time 150 ms; turbo factor 7; matrix 253×384; and 1 acquisition, a turbo T2-weighted axial sequence, 80 sections; each section 2 mm, no gap, 340-mm field of view; TR 8870/146; turbo factor 19; matrix 384×512; and 1 acquisition]. Dynamic FLASH 3-D (three-dimensional fast low-angle shot) contrast-enhanced series were performed using the following parameters: radiofrequency spoiled gradient-echo; no fat suppression; 5 measurements (series); 80 sections; each section 2 mm at 2-mm intervals; matrix 384×512; 340-mm field of view; 10/4.5; flip angle 25°; parallel imaging factor of 2, and 1 acquisition (measurement). The scanning time was 2 min 6 s per series time point. The first time point was acquired before contrast administration. During a subsequent pause of 25 s, a single dose of gadopentetate dimeglumine (0.1 mmol/kg, Magnevist, Berlex, Montville, NJ, USA) was injected at a rate of 2 ml/s and was immediately followed by a 20-ml normal saline flush injected at a rate of 1 ml/s. Series 2–5 were then acquired sequentially with no interscan delays. Initial and delayed dynamic images were obtained within 8 min after the injection of contrast material. Centric spatial encoding was used for all sequences.

PEM/WBPET image acquisition

Patients were required to fast for 4–6 h. The fasting blood glucose was measured and those with levels less than 7.8 mmol/l (mean=5.4 mmol/l, range 3.6–7.7 mmol/l) were injected with FDG (370 MBq, median dose 432.9 MBq, range 344.1–577.2 MBq). Patients were asked to rest quietly for 60 min (mean=77, range 26–208 min) to allow the radiotracer to circulate after which bilateral 10-min craniocaudal (CC) and mediolateral oblique (MLO) acquisitions were obtained with the Naviscan PEM scanner (Naviscan, Inc., San Diego, CA, USA) (see Fig. 1a, b). Additional views (axillary, cleavage, or mediolateral, axillary tail, lateral) were obtained at the discretion of the physician (refer to www.naviscan.com/positioning).

WBPET images were obtained immediately following PEM imaging (approximately 122 min after radiotracer injection) with the patient lying in the supine position using a Siemens CTI/HR+WBPET (Siemens Medical Solutions, Malvern, PA, USA); 7-min emission/3-min transmission acquisitions from the base of the skull to the upper thigh were obtained. The transmission scans were interleaved between multiple emission scans to correct for nonuniform attenuation. The images were reconstructed using an iterative reconstruction algorithm and both attenuation-corrected and non-attenuation-corrected images were interpreted visually. Slice thickness and slice interval were both 4 mm.

Image interpretation

Mammograms, MRI, and PEM images were reviewed by one of six rotating Mammography Quality Standards Act certified radiologists at the Boca Raton Regional Hospital. All examinations were interpreted according to the American College of Radiology Breast Imaging Reporting and Data System (BI-RADS) with BI-RADS 4 and above treated as suspicious for malignancy. Physicians were requested to

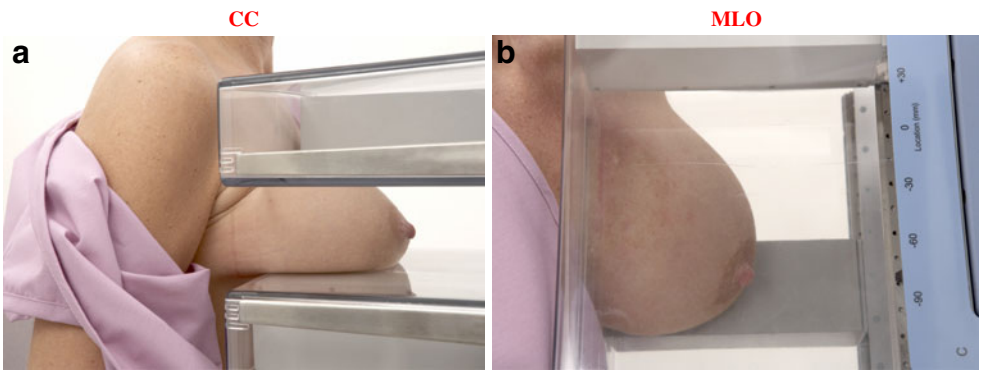

Fig. 1 Positioning of subjects in the PEM scanner for image acquisition in the CC and MLO positions are shown in **a** and **b**, respectively

review the image with access to conventional imaging (mammography or ultrasound) but without influence of the alternative (PEM versus MRI) imaging modality. WBPET images were reviewed in three orthogonal planes on a dedicated PET workstation and interpreted by a board certified nuclear physician who did not have access to PEM images. Relevant demographic, clinical history, image interpretation, biopsy, and final surgical pathology information was collected using case report forms.

Quantitative FDG uptake

A ratio of FDG uptake between the lesion in question and the background glandular tissue was used to determine the risk assessment of malignancy on PEM images. First, a region of interest (ROI) was drawn including normal ipsilateral breast tissue and the average or mean called a PEM uptake value was recorded (PUV_{mean}). Next an ROI was drawn around the lesion in question and the maximum FDG uptake (PUV_{max}) recorded. The ratio of the PUV_{max} of the lesion to the PUV_{mean} of the background (LTB) was calculated and recorded. The architectural distribution of FDG uptake, i.e., focus, linear or ductal, mass, non-mass distribution etc., and LTB was used to determine the assessment according to a proposed PEM lexicon based on MRI Breast Imaging Reporting and Data System (BI-RADS) [23] and was provided to investigators as part of their PEM interpretive training. Briefly, an LTB ratio of 2.0 and focal localization was considered suggestive of malignancy warranting biopsy or BI-RADS 4 categorization [24, 25]. An LTB ratio less than 1.5 was considered most likely benign and ratios between 1.5 and 2.0 were rated as suspicious dependent on the architecture for FDG uptake.

Lesions seen on WBPET were localized and the maximum standardized uptake value (SUV_{max}) was used to determine malignancy. An ROI was drawn around the abnormality and the SUV recorded in the clinical report. The SUV_{max} has been shown to be significantly influenced by histological grade, invasiveness, and hormonal receptor status of the primary tumor [26, 27].

Final surgical histopathological correlation of index and ipsilateral lesions

Approximately 3 weeks after PEM and WBPET (mean= 18.9±15.1 days, min.=1 day, max.=110 days), patients underwent surgery for excision of the primary tumor. Final surgical pathology was classified as *invasive carcinoma* [invasive lobular carcinoma (ILC), invasive ductal carcinoma (IDC), invasive tubulolobular carcinoma (ITLC), invasive micropapillary carcinoma (IMPC)], *in situ carcinoma* [ductal carcinomas in situ (DCIS) or Paget's disease], *high risk* [atypical ductal hyperplasia (ADH), atypical lobular hyperplasia (ALH)], or *benign pathology* [fatty necrosis, inflammation (biopsy site), fibrocystic change (FCC)].

Index lesion size on imaging was compared to size on surgical pathology. The largest diameter in each case was used to calculate lesion size. Ipsilateral lesions were classified as *invasive and in situ carcinoma* (IDC, ILC/ITLC, IDC/ILC/DCIS, IDC/DCIS, DCIS), *high risk* [ADH, ALH, lobular carcinoma in situ (LCIS)], or *benign* [fibroadenoma (FA), FCC].

Data collection and image analysis

The sensitivity was calculated for each modality based on interpretations for 182 index lesions. The sensitivity, specificity, and accuracy were calculated for the 67 additional ipsilateral lesions. Abbreviations were as follows: N, number of patients; TP, true-positive; TN, true-negative; FN, false-negative; FP, false-positive. If the final pathology for index lesions showed no residual carcinoma, the lesions were classified as "FP" if they were depicted as carcinoma on the imaging modality or "TN" if they were not seen on the imaging modality. Sensitivity was calculated using the following formula: TP/(TP + FN). For additional ipsilateral lesions, the following formulas were used for calculation of specificity: TN/(FP + TN); accuracy: (TN + TP)/(TN + TP + FN + FP); positive predictive values (PPV): TP/(TP + FP); and negative predictive values (NPV): TN/(FN + TN). Performance characteristics were expressed as percentages.

Statistical analysis

The data were presented as mean ± standard deviation (SD). Stata software (StataCorp LP, College Station, TX, USA) was used for statistical analysis and p values less than 0.05 were considered to represent a significant difference between two populations. The 95% confidence intervals (CI) for the binary test measures (sensitivity, specificity, and accuracy) were calculated using exact binomial confidence intervals. McNemar's test was performed on comparisons of the same group of cases when comparing different imaging modalities (comparison of performance between PEM and WBPET or PEM and MRI or MRI and WBPET). Chi-square tests were used to evaluate the effect of breast density, menopausal status, and HRT use on the sensitivity of PEM and MRI. Spearman's rank correlation coefficient was used to measure the correlation between size and histology. No adjustments were made for multiple comparisons.

Results

Demographics and relevant clinical history

In the study, 250 patients were approached, 11 declined and 239 patients were enrolled. A total of 31 were subsequently disqualified: 2 because they did not have a primary breast malignancy, 17 because they received neoadjuvant chemotherapy prior to surgical intervention, 3 due to incomplete imaging (1 refused MRI imaging and 2 subjects withdrew from the study), and 9 were disqualified because they had no final surgical pathology due to withdrawal from the study center. An additional 26 patients were ineligible because the MRI or PEM imaging was performed before study entry, leaving a total of 182 analyzable patients (87.5%, 182/208) (Table 1). One hundred sixty-seven women had residual tumor at surgery.

The demographics and relevant clinical history of patients enrolled, analyzed, and who had residual tumor on final surgery are summarized in Table 2. The demographics were similar across the patient groups. Of the 182 patients that were analyzable, 26.4% (48/182), 7.1% (13/182), and 66.0% (120/182) were pre-, peri-, and postmenopausal, respectively, and 48.4% (88/182) had extreme or heterogeneously dense breast tissue. The majority of patients had not used HRT (63.7%, 116/182), while 61 of 182 (33.5%) subjects did have a history of HRT use prior to inclusion in the study.

Histopathology of biopsied lesions

Of the lesions studied, 45.6% (83/182) were clinically palpable and 54.4% (99/182) were not. The majority of the lesions (91.8%; 167/182) were sampled using a vacuum-assisted core biopsy approach and the remainder had excision, punch/shave, fine-needle aspiration, and unknown biopsy procedures, respectively (Table 3). Pathology showed that *invasive disease* was found in 77.5% (141/182) of patients and DCIS (20.9%) and Paget's disease (1.6%) was found in 22.5% (41/182).

Table 1 Participant enrollment summary

Participant summary	Number of participants
Subjects approached	250
Subjects who declined participation	11
Subjects enrolled	239
Ineligible because did not have primary breast malignancy	2
Disqualified due to treatment with neoadjuvant chemotherapy	17
Disqualified due to failure to complete imaging protocol	3
Disqualified due to lack of final pathology	9
Subjects with complete data	208
Disqualified because MRI or PEM was performed prior to study entry	26
Analyzable subjects	182
Subjects with residual tumor at final pathology	167

Index lesion image analysis

Both PEM and MRI had an index lesion detection sensitivity of 92.8% (95% CI, range 88–96%, N=182) and both were significantly better than the 67.9% (95% CI, range 60–70%, N=173) sensitivity obtained with WBPET (p<0.001, McNemar's test). Nine subjects did not undergo WBPET imaging. There was no significant difference in the sensitivity between PEM and MRI (p=NS, McNemar's test).

Table 4 summarizes the sensitivity as categorized by tumor stage in the 167 subjects who had residual cancer at final surgical treatment. The other 15 had no cancer found at final surgery. Of these 167 index lesions, 30 were DCIS, and PEM detected 90.0% (27/30), while MRI detected 83.0% (25/30) (p=NS). One hundred and thirty-seven index lesions were invasive cancer of which PEM detected 93.4% (128/137), while MRI detected 94.9% (130/137) (p=NS). Both modalities have comparable sensitivity in depiction of invasive cancer of different sizes (1 mm to >50 mm), while the sensitivity of PEM was 100.0% for T1a invasive cancer in this small series. The imaging concordance with specific pathology is summarized in Table 5. There were 137 invasive cancer cases, 30 in situ, 4 high risk, and 11 benign. The sensitivities of PEM and MRI for invasive carcinoma were comparable (PEM=93.4% and MRI=94.9%). PEM however was slightly more sensitive in the detection of

Table 2 Participant demographics

Characteristic	Enrolled participants, *N*=208 (%)	Analyzed participants, *N*=182 (%)	Participants with residual tumor at final pathology, *N*=167 (%)
Race			
White	194 (93.3)	168 (92.3)	155 (92.8)
African American	1 (0.5)	1 (0.6)	1 (0.6)
Asian	2 (1.0)	2 (1.1)	1 (0.6)
Other/unknown	11 (5.3)	11 (6.0)	10 (6.0)
Menopausal status			
Premenopausal	52 (25)	48 (26.4)	42 (25.2)
Perimenopausal	17 (8.2)	13 (7.1)	12 (7.2)
Postmenopausal	138 (66.4)	120 (66.0)	112 (67.0)
Unknown	1 (0.5)	1 (0.5)	1 (0.6)
History of HRT			
No	132 (63.5)	116 (63.7)	106 (61.7)
Yes	71 (34.1)	61 (33.5)	57 (34.1)
Unknown	5 (2.4)	5 (2.8)	4 (2.4)
Previous history of breast cancer			
No	187 (89.9)	169 (92.9)	156 (93.4)
Yes	21 (10.1)	13 (7.1)	11 (6.6)
Participants with implants			
No	189 (90.9)	166 (91.2)	153 (91.6)
Yes	19 (9.1)	16 (8.8)	14 (8.4)
Breast density			
Extremely dense	15 (7.2)	13 (7.1)	12 (7.2)
Heterogeneously dense	88 (42.3)	75 (41.2)	70 (41.9)
Scattered fibroglandular	89 (42.9)	80 (44.0)	71 (42.5)
Fatty	10 (4.8)	9 (5.0)	9 (5.4)
Unknown	6 (2.9)	5 (2.7)	5 (3.0)

benign or atypical findings for patients with no residual tumor at index lesion site (sensitivity of PEM=72.7% vs MRI=54.6%).

The sensitivities for index lesion depiction when categorized by menopausal status, breast density, and HRT use are summarized in Table 6. Neither menopausal status nor breast density affected lesion detection sensitivity of either PEM or MRI ($p>0.05$, chi-square test). Although PEM was very similar to MRI in the depiction of cancer lesions, there were some cases where PEM appeared to be more sensitive. For example a 62-year-old woman who had a history of using HRT presented with a 1.8-cm ill-defined solid mass at 4 o'clock in the right breast by mammography that was diagnosed at pathology to be invasive mammary carcinoma with lobular features (grade I). The lesion was clearly detected in the right breast by PEM, but missed by MRI (Fig. 2a). As shown in the PEM images (Fig. 2b, c), a focal area of increased FDG activity corresponding to the biopsy-proven malignancy in the inner lower quadrant approximately 1 cm from the nipple and measuring approximately 1.3×0.8×0.5 cm was clearly observed.

Final surgical pathology of all index lesions is summarized in Table 7. Final surgical pathology confirmed that 75.0% (137/182) of the index lesions were invasive cancer with 16.5% carcinoma in situ (30/182) and 2.2% (4/182) were considered high risk lesions with presumably the original cancer removed at biopsy. Six percent (11/182) were found to be residual benign processes such as inflammation, fat necrosis, or FCC. The difference in the number of invasive cancers between the final surgical pathology results and biopsy results is presumed to reflect the complete removal of the malignancy at biopsy and post-biopsy inflammatory changes.

The size range of the invasive index tumors as measured by PEM and MRI were compared to the final surgical specimen as shown in Table 8. The average, median, and minimum sizes of the lesions identified by MRI, PEM and surgical pathology showed similar values. Spearman's correlation coefficients for size on imaging vs. histopathology were 0.61 for both PEM and MRI. However, PEM tended to overestimate the size in the largest lesion compared to surgical pathology and MRI

Table 3 Summary of index lesion characteristics, type of biopsy, and histopathology prior to study entry in 182 analyzable subjects with known cancer

Characteristics	Patients, *N*=182 (%)
Palpable lesion	
Yes	83 (45.6)
No	99 (54.4)
Type of biopsy	
Core	167 (91.8)
Excisional biopsy	3 (1.7)
Punch/shave	2 (1.1)
Fine-needle aspiration	5 (2.7)
Unknown	5 (2.7)
Biopsy pathology	
Invasive disease	141 (77.5)
IDC	89 (48.9)
IDC+DCIS	21 (11.6)
IDC+ILC	4 (2.2)
ILC/ITLC	22 (12.1)
ILC+DCIS	1 (0.5)
Breast cancer (unknown type)	3 (1.7)
Intracystic papillary carcinoma	1 (0.5)
DCIS and Paget's disease	41 (22.5)
DCIS	38 (20.9)
Paget's disease	3 (1.7)

IDC invasive ductal carcinoma, *DCIS* ductal carcinoma in situ, *ILC* invasive lobular carcinoma, *ITLC* invasive tubulolobular carcinoma

[*maximum lesion size (mm)*: surgical pathology=95.0, PEM=120, MRI=95.0].

A total of 12 lesions were missed on both MRI and PEM imaging and classified as "FN." For all PEM cases, competition from high glucose levels could not explain these findings as review of the blood glucose levels showed

Table 4 PEM and MRI sensitivity for depicting known cancers in 167 subjects with residual tumor at final pathology, grouped by tumor type and size

Index lesions (*N*=167)	PEM, % (*N*/*N*)	Breast MRI, % (*N*/*N*)
DCIS (*N*=30/167)	90.0 (27/30)	83.0 (25/30)
Invasive cancer (*N*=137/167)	93.0 (128/137)	95.0 (130/137)
T1a (*N*=4)	100.0 (4/4)	75.0 (3/4)
T1b (*N*=21)	85.7 (18/21)	90.5 (19/21)
T1c (*N*=57)	93.0 (53/57)	94.7 (54/57)
T2 (*N*=52)	96.2 (50/52)	98.1 (51/52)
T3 (*N*=3)	100.0 (3/3)	100.0 (3/3)

DCIS ductal carcinoma in situ, *T1a* tumor >1 mm but ≤5 mm, *T1b* tumor >5 mm but ≤10 mm, *T1c* tumor >10 mm but ≤20 mm, *T2* tumor >20 mm but ≤50 mm, *T3* tumor >50 mm

Table 5 PEM and MRI sensitivity for depicting known cancer index lesions in 182 analyzable subjects, grouped by histopathology at final treatment surgery

Pathology at surgery		Total *N* (%)	PEM sensitivity *N* (%)	MRI sensitivity *N* (%)
Invasive cancer		137 (75)	128 (93)	130 (95)
	IDC	56 (31)	55 (98)	51 (91)
	IDC-DCIS	53 (29)	50 (94)	53 (100)
	ILC	20 (11)	16 (80)	18 (90)
	IDC ILC	1 (0.6)	1 (100)	1 (100)
	IDC, ILC, DCIS	1 (0.6)	1 (100)	1 (100)
	ILC, DCIS	2 (1)	1 (50)	2 (100)
	ITLC	3 (2)	3 (100)	3 (100)
	IMPC	1 (0.6)	1 (100)	1 (100)
In situ carcinoma		30 (17)	27 (90)	25 (83)
	DCIS	28 (15)	26 (93)	23 (82)
	DCIS with Paget's	2 (1)	1 (50)	2 (100)
High risk		4 (2)	2 (50)	2 (50)
	ADH	3 (2)	1 (33)	2 (67)
	ALH	1 (0.6)	1 (100)	0 (0)
Benign		11 (6)	8 (73)	6 (55)
	Fat necrosis	4 (2)	3 (75)	2 (50)
	FCC	1 (0.6)	1 (100)	1 (100)
	Biopsy site	6 (3)	4 (67)	3 (50)
Total positive cases		167 (92)	155 (93)	155 (93)
Total negative cases[a]		15 (8)	10 (67)	8 (53)

IDC invasive ductal carcinoma; *DCIS* ductal carcinoma in situ; *ILC* invasive lobular carcinoma; *ITLC* invasive tubulolobular carcinoma; *IMPC* invasive micropapillary carcinoma; *ADH* atypical ductal hyperplasia; *ALH* atypical lobular hyperplasia; *FCC* Fibrocystic changes

[a] In 15/182 cases, final histopathology was benign, leaving 167 lesions with residual cancer. PEM and MRI both depicted 155/167 known cancer lesions with an index lesion depiction sensitivity of 92.8%. For pure DCIS lesions, PEM sensitivity was 93% (26/28), while MRI was 82% (23/28)

that all were below the 7.8 mmol/l requirement, with an average value of 5.6 mmol/l. On further review it was determined that 3 of 12 "FN" PEM index lesions were missed due to poor patient positioning (cases: 1 ILC, 1 IDC/DCIS, and 1 IDC), such that the portion of the breast with the lesion was not included in the field of view. Of the 12 cases, 8 had low FDG uptake (cases: 3 DCIS, 3 ILC, and 2 IDC/DCIS) and the final FN PEM case was a 3 mm lesion (ILC). Review of FN PEM images of these nine cases found that four of these images could be identified in retrospect of which three were in patients with bilateral breast implants. Of the three cases with bilateral implants, DCIS was present in two cases and IDC was found in a

Table 6 PEM and MRI lesion depiction accuracy for 182 index lesions, grouped by different menopausal status, breast densities and history of HRT use

Category	182 patients analyzed *N* (%)	PEM accuracy *N* (%)	MRI accuracy *N* (%)
Menopausal status			
Premenopausal	48 (26)	42/48 (88)	41/48 (85)
Perimenopausal	13 (7)	12/13 (92)	13/13 (100)
Postmenopausal	120 (66)	105/120 (88)	107/120 (89)
Unknown	1 (0.5)	1/1 (100)	1/1 (100)
Breast density			
Extreme density	13 (7)	10/13 (77)	9/13 (69)
Heterogeneous density	75 (41)	66/75 (88)	67/75 (89)
Scattered fibroglandular	80 (44)	71/80 (89)	74/80 (93)
Fatty	9 (5)	8/9 (89)	8/9 (89)
Not listed	5 (2.7)	5/5 (100)	4/5 (80)
History of HRT			
No	116 (64)	102/116 (88)	104/116 (90)
Yes	61 (34)	54/61 (89)	53/61 (87)
Unknown	5 (2.8)	4/5 (80)	5/5 (100)

Chi-square was used to evaluate the effect of menopausal status on the accuracy of the imaging modalities; $p=0.84$ for PEM (*NS*), $p=0.45$ for MRI. Chi-square was used to evaluate the effect of breast density on the accuracy of the imaging modalities; $p=0.38$ for PEM (*NS*), $p=0.39$ for MRI. Chi-square was used to evaluate the effect of HRT use on the accuracy of the imaging modalities; $p=0.7$ for PEM (*NS*), $p=0.46$ for MRI

single case, and all had asymmetric FDG uptake beyond the implant surface when compared to the contralateral breast. In retrospect these cases were suspicious for malignancy; however, they were interpreted as asymmetric implant-induced capsular fibrosis. The single IDC case was appreciated in retrospect and it is unclear why it was missed on the original interpretation. Of the remaining five of nine lesions, one lesion was 1 mm in size as determined by pathology, three cases were ILC of which two were also not seen on MRI, and finally, one case was "only faintly" seen on MRI due to its proximity to the biopsy clip and pathology revealed that the majority of this lesion had been removed at biopsy which may explain why it was not visualized on PEM.

Ten cases were classified as FP on PEM and eight cases were classified FP using MRI. Two lesions, one ADH and one ALH, were identified by PEM. MRI identified two lesions of ADH that were classified as FP also. Both of these are high risk pathologies and their identification is potentially important in patient management decisions. Other findings resulting in FP results for both PEM and MRI were: Fat Necrosis (three and two, respectively), FCC (same single lesion for both PEM and MRI), and biopsy site (four lesions on PEM and three on MRI).

Additional ipsilateral lesion image analysis

Of the 182 analyzable patients, a total of 74 additional ipsilateral lesions were found in 35% (63/182) of patients. Table 9 summarizes the time of lesion sampling relative to the PEM or MRI imaging. Seven patients had sampling interventions done after MRI and before PEM were eliminated from further analysis, leaving a total of 67 additional ipsilateral lesions for analysis. Performance characteristics (sensitivity, specificity, accuracy, PPV and NPV using final histopathology as the "truth") of the two modalities are shown in Table 10, and Table 11 summarizes the final surgical pathology of the ipsilateral lesions. An

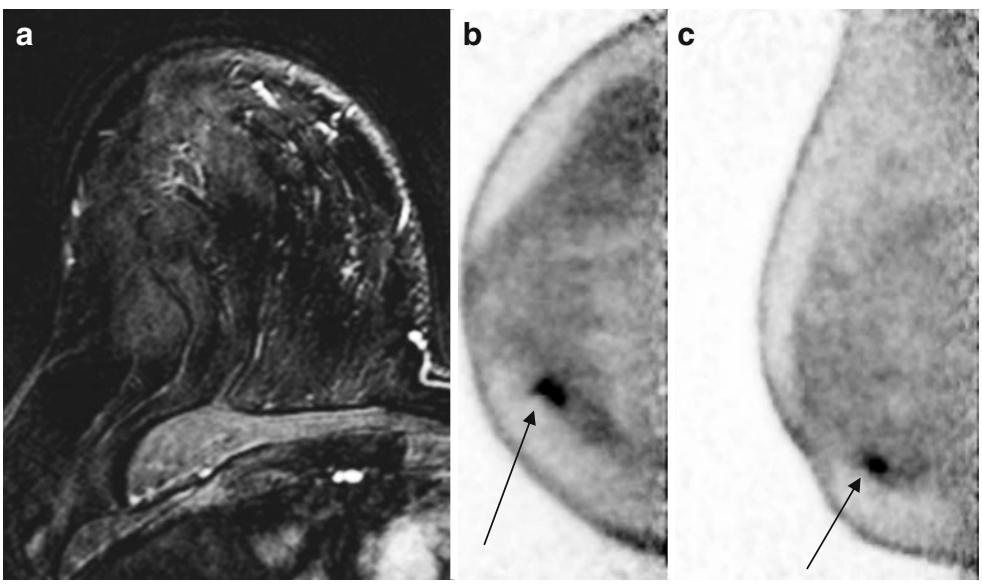

Fig. 2 A 62-year-old female patient presented with a 1.8-cm ill-defined solid mass at 4 o'clock in the right breast by mammography that was diagnosed at pathology to be invasive mammary carcinoma with lobular features (grade I). MRI failed to detect any suspicious lesions in the right breast (**a**). **b**, **c** On PEM, a focal area of increased FDG activity corresponding to the biopsy-proven malignancy in the right breast and the inner lower quadrant approximately 1 cm from the nipple and measuring approximately 1.3×0.8×0.5 cm was clearly observed (*arrows*)

Table 7 Comparison of biopsy and final surgical histology for 182 index lesions

Pathology	Biopsy before study entry *N*=182 (%)	Final surgical pathology *N*=182 (%)
Invasive carcinoma	141 (77.5)	137 (75.3)
IDC	89 (48.9)	56 (30.8)
IDC+DCIS	21 (11.6)	53 (29.1)
ILC/ITLC	22 (12.1)	23 (12.6)
IDC+ILC	4 (2.2)	1 (0.5)
ILC+DCIS	1 (0.5)	2 (1.1)
IDC+ILC+DCIS	–	1 (0.5)
IMPC	–	1 (0.5)
Breast cancer (unknown type)	3 (1.7)	–
Intracystic papillary ca.	1 (0.5)	–
In situ carcinoma	41 (22.5)	30 (16.5)
DCIS	38 (20.8)	28 (15.4)
DCIS+Paget's disease	–	2 (1.1)
Paget's disease	3 (1.7)	–
High risk	–	4 (2.2)
ADH/ALH/LCIS		4 (2.2)
Benign pathology	–	11 (6.0)
Fat necrosis	–	4 (2.2)
Inflammation (biopsy site)	–	6 (3.3)
FCC		1 (0.5)

IDC invasive/infiltrating ductal carcinoma; *DCIS* ductal carcinoma in situ; *ILC* invasive lobular carcinoma; *ITLC* invasive tubulo-lobular carcinoma; *ADH* atypical ductal hyperplasia; *LCIS* lobular carcinoma in situ; *ALH* atypical lobular hyperplasia; *IMPC* invasive micropapillary carcinoma; *FCC* fibrocystic change. (–) Not assessed

example case where multifocal disease was seen equally well on PEM and MRI is shown in Fig. 3.

Of the 40 malignancies in 67 additional lesions, PEM depicted 34 with a sensitivity of 85%, while MRI depicted 39 with sensitivity of 98%. (P value=0.074). Six cases were categorized as FN on PEM imaging, while one case was categorized as FN by MRI. For PEM imaging, three lesions had poor FDG uptake (two IDC and one ILC) and could not be appreciated on retrospective evaluation. One FN lesion was missed due to poor patient positioning (ILC) as the lesion was not within the field of view. One case, ITLC, was < 1mm in size and was missed on both PEM and MRI, while the second case, DCIS, was a small focus found at pathology.

Of the 27 benign lesions among 67 additional lesions, PEM specificity was 74% (20/27) while that of MRI was 48% (13/27)[P value=0.096]. A total of 14 FP ipsilateral lesions were seen on MRI, while only 7 were seen on PEM. Both PEM and MRI each identified a single case of ADH which was classified as FP, but its identification is important and could change surgical planning. Three FAs, one papilloma, and two cases of FCC were categorized as FP on PEM. MRI had an additional five cases with FA and eight with FCC listed in this category. No statistically significant difference was found between the accuracy of PEM and MRI in ipsilateral lesion depiction (p=0.81, McNemar's test), PPV, or NPV.

Discussion

In the USA an estimated 194,280 new cases of breast cancer are diagnosed each year with an estimated 40,610 annual deaths [28]. In addition, approximately 1 million surgical and needle breast biopsies a year are performed on benign tissue with a frequent occurrence of additional operations for positive or close surgical margins on partial mastectomy patients [3]. Precise and accurate imaging technology may improve the accuracy of partial mastectomies and develop consistent strategies for presurgical management. Although a relatively new technology, several studies have reported the sensitivity, specificity, and accuracy of PEM in detection of breast cancer lesions [21, 29–31]. Overall, these series have shown good specificity (86%) and sensitivity (90%) and are predicted to be better than WBPET scanners. However, to date, none of these studies have directly compared PEM with MRI and WBPET imaging within the same patient population.

The present trial demonstrates that PEM has comparable sensitivity to MRI in depiction of index and ipsilateral lesions. The sensitivity of MRI and PEM were both 92.8% for index lesions and for depiction of additional unsuspect-

Table 8 Index lesion size of invasive tumors (*N*=114)

	Average lesion size (mm±SD)	Median lesion size (mm)	Minimum lesion size (mm)	Maximum lesion size (mm)
Surgical pathology	20.6±13.9	18.0	4.0	95.0
PEM	19.6±14.1	17.5	3.0	120.0
MRI	19.7±12.5	18.0	2.0	95.0

Only invasive tumors where the largest tumor diameter was reported for PEM, MRI and final treatment surgery were included in this analysis. DCIS lesions and those with no residual tumor at surgery were excluded in this analysis

Table 9 Time of ipsilateral lesion sampling relative to PEM and MR imaging

Time of lesion sampling	Number of ipsilateral lesions (%)	Number of additional ipsilateral lesions (%)
After PEM & MRI	24 (83.0)	5 (17.0)
Before PEM & MRI	34 (89.0)	4 (11.0)
After MRI before PEM	5 (71.0)	2 (29.0)
Total	63 (85.0)	11 (15.0)

74 ipsilateral lesions were identified in 63 patients. Of these 7 lesions were biopsied between PEM and MRI imaging and therefore excluded from final analysis. A total of 67 ipsilateral lesions in 58 patients were included in the ipsilateral lesions analysis. Note: 38 analyzed lesions were biopsied prior to PEM and MRI, including 24 malignancies. For lesions biopsied after PEM and MRI imaging, PEM sensitivity was 71% (12/17) and MRI sensitivity was 94% (16/17)

ed ipsilateral lesions, the sensitivity of PEM was 85.0% and 97.5% for MRI, and were not significantly different from each other. The high sensitivity of MRI for index and ipsilateral lesions in this study is on the high end of the reported 85–100% range [6]. This high sensitivity is most likely due to inclusion of known malignancies in sensitivity analyses, and the fact that 38/67 additional ipsilateral lesions had been biopsied prior to imaging. Both MRI and PEM had comparable sensitivities for DCIS and for invasive cancer of various stages. Final surgical pathological analysis of invasive tumors, excluding DCIS and lesions with no malignancy, confirmed that PEM and MRI were good in prediction of average, median, and minimum size lesions, though PEM tended to overestimate the largest lesion detected compared to surgical pathology and MRI. This may be a result of the limited tomography of PEM imaging where the number of projections is constrained by the limited angular sampling capable with planar detectors. Like PEM, others have shown that with both ultrasound and MRI disease extent is not infrequently overestimated in

Table 10 Performance characteristics of PEM and MRI for 40 additional ipsilateral malignancies among 67 biopsied breast lesions

Modality	PEM (%) [95%CI]	MRI (%) [95%CI]	*P*-Value
Sensitivity	34/40 (85) [70 to 94]	39/40 (98) [89 to 100]	0.074
Specificity	20/27 (74) [54 to 89]	13/27 (48) [29 to 68]	0.096
Accuracy	54/67 (81) [69 to 89]	52/67 (78) [66 to 87]	0.81
PPV *(biopsies recommended)*	34/41 (83)	39/53 (74)	
NPV	20/26 (77)	13/14 (93)	

McNemar's test was used to check equality of sensitivity and specificity of the two modalities and were not significantly different

Table 11 Summary of ipsilateral lesion histopathology at biopsy for 67 additional ipsilateral lesions

Histopathology	Lesion *N* (%) *N*=67	PEM sensitivity (%)	MRI sensitivity (%)
Invasive and in situ carcinoma	40 (60)	34 (85)	39 (98)
IDC	18 (27)	16 (89)	18 (100)
ILC/ITLC	5 (8)	2 (40)	4 (80)
IDC/ILC/DCIS	1 (2)	1 (100)	1 (100)
IDC/DCIS	10 (15)	10 (100)	10 (100)
DCIS	6 (9)	5 (83)	6 (100)
High risk	2 (3)	1 (50)	1 (50)
ADH	2 (3)	1 (50)	1 (50)
Benign	25 (37)	6 (24)	16 (64)
BBT	3 (5)	0 (0)	0 (0)
FA	7 (10)	3 (43)	5 (71)
FCC	15 (22)	3 (20)	8 (53)

IDC invasive/infiltrating ductal carcinoma; *DCIS* ductal carcinoma in situ; *ILC* invasive lobular carcinoma; *ITLC* invasive tubule-lobular carcinoma; *ADH* atypical ductal hyperplasia; *BBT* benign breast tissue; *FA* fibroadenoma; *FCC* fibrocystic change

12–29% of patients, respectively, resulting in potentially unnecessary mastectomy [32]. However, if two different imaging approaches such as anatomic (MRI) and functional or metabolic (PEM) identify the same abnormalities, greater confidence and accuracy should result as shown in Fig. 3, an example of multifocal disease. For ipsilateral lesions, MRI had a trend towards better sensitivity compared to PEM while PEM trended to have greater specificity compared to MRI, however neither reached statistical significance (p=0.074 and p=0.096 respectively). The specificity of MRI is reported to vary between 37 and 100% [6]. Ipsilateral lesion specificity in this study was within this range at 48% for MRI while that of PEM was 75%.

The major substudy analysis of the current investigation was to compare the sensitivity of PEM and MRI for depiction of index lesions in women with different menopausal status, various breast densities, and with a history of HRT use. These analyses were an important inclusion to our study design since background breast density and hormonal status are two factors that have challenged mammography and MRI breast imagers when it comes to cancer detection [3, 7, 13]. Others have shown a benefit of metabolic imaging with FDG in cancer detection in these situations. For example, studies by Vranjesevic et al. [33] and Kumar et al. [34] both reported that FDG uptake increases significantly with breast density, but they concluded that the highest background levels seen would not be sufficient to interfere with lesion detection. But it is clear from previous studies [35] that for MRI, FP findings increase during a patient's menstrual cycle due to hormonal

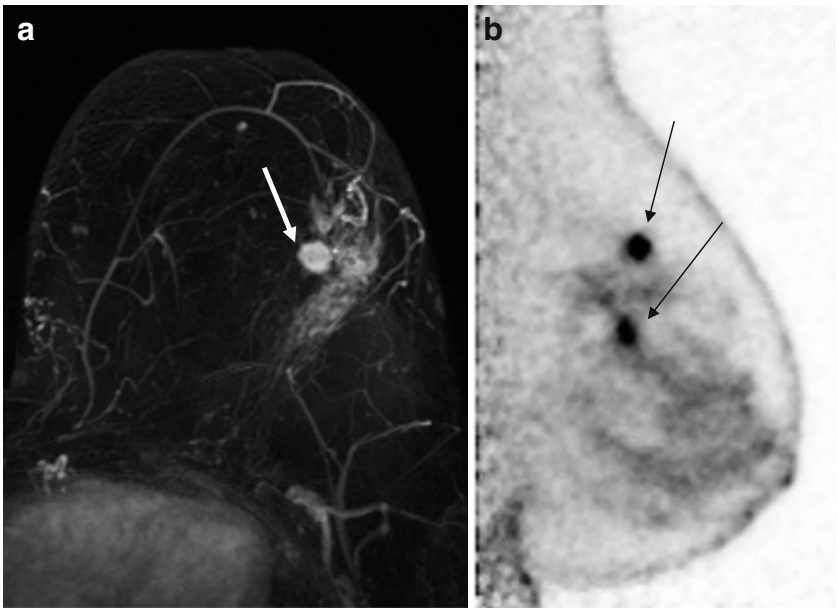

Fig. 3 A 61-year-old subject presented with an area of clustered pleomorphic microcalcifications in the upper outer quadrant of the left breast which proved to be DCIS following stereotactic biopsy. An ultrasound confirmed the presence of the biopsy clip and identified an additional solitary 7-mm nodule in the same quadrant. Core sampling found this nodule to be IDC. MRI identified a 1.2-cm irregular enhancing mass (depicted by *arrow*) with a possible satellite lesion (**a**). PEM confirmed a 1.1×1.0×2.2-cm mass with a second 0.7×0.7×2.5-cm inferior mass with final pathology confirming IDC and DCIS, respectively (**b**), as depicted by *arrows*

influences on breast tissue. Analysis of variance on lesion detection versus breast density or menopausal status in this study did not find any significant influence of breast density and menopausal status for either PEM or MRI imaging, and these data suggest that PEM is an attractive alternative imaging approach in women with dense breast tissue or who are pre- or perimenopausal. A recent study by Mavi et al. [36], involving 250 patients with newly diagnosed breast cancer of a similar age group to this study (50.9±9.7 years), showed that FDG uptake decreases as age increases and breast density decreases. Importantly, they found menopausal state had no effect on FDG uptake, which supports our finding of no change in PEM accuracy with menopausal status. With respect to HRT status, a growing body of evidence suggests that there is an association between the use of HRT and a higher risk of both ILC and invasive-lobular mixed carcinoma [7]. The data presented here show that PEM is equivalent to MRI for the detection of index cancers in the 61 subjects who had a history of using HRT prior to study inclusion (p=NS). For ILC, PEM depicted 16 of 20 cases (80% sensitivity) in contrast to 18 of 20 depicted by MRI (90% sensitivity), suggesting that the two modalities are comparable for ILC depiction.

The sensitivity of PEM and MRI with WBPET in presurgical planning for women with known breast cancer was also compared. Although FDG WBPET has proven to be highly useful in the diagnosis and staging of a variety of malignancies, for breast cancer, its sensitivity ranges between 64 and 96%, with an average of 74% across multiple studies [37]. The reason for this lower sensitivity is partially due to both the small size of the cancer at detection and the lower levels of FDG uptake found in different types of breast cancer. Preliminary evaluation of PEM for index lesions found a sensitivity of 90% for invasive malignancies and 91% sensitivity for DCIS [21]. This shows a substantial improvement for DCIS when compared to the 10% WBPET sensitivity found by Avril et al. [38]. In the current study, PEM and MRI had an index lesion detection sensitivity of 92.8% which was significantly better than the 68% found with WBPET (p>0.0001). Studies on dual time point imaging WBPET have clearly shown improved discrimination between malignant and benign processes [39] as well as improved discrimination between noninvasive and invasive breast cancers [40] with delayed times at imaging. Since PEM imaging was done first, WBPET should have had the detection advantage [40], all else being equal.

We also performed analysis of FN cases. Previous PET studies had found that certain early breast tumors, with less biologically aggressive features, were less glycolytic and could evade WBPET detection due to insufficient FDG uptake [41]. Review of the FN PEM cases in this study found that 11 or 4.4% of the total lesions (index + ipsilateral) were not visualized due to "lack of FDG uptake." Although many were identified in retrospect, of those that were not, many were small. Thus, the question of whether these small lesions could have been detected if PEM imaging had been done at a later time when the contrast of the lesion increases remains unanswered. To this point, the PEM scanner manufacturer currently recommends waiting 90 min post-injection of FDG for all PEM-guided biopsies, specifically to take advantage of the improved lesion detection that is found at this later time.

Collectively, the data in the present study suggest that PEM can be used as an adjunct or alternative imaging

modality to MRI in presurgical management of breast cancer patients, which is an important finding since many patients cannot and will not have a breast MRI for many reasons [8–16]. The American College of Radiology Imaging Network 6666 US Screening Protocol recently published a study of 1,215 women with elevated breast cancer risk who could, according to protocol guidelines, undergo breast MRI [42]. In spite of this, only 57.9% of the eligible patients agreed to participate with claustrophobia being the major reason for refusal (25.4%). The other reasons for declining an MRI in consecutive order were time constraints, financial concern, no physician referral, lack of interest, medically intolerant to MRI, refusal of intravenous injection, probable additional biopsy procedures as a result of an MRI, scheduling constraints within a patient's menstrual cycle and their hormonal status, travel, gadolinium-related risks or allergies, and finally unknown reasons. It is important to note that claustrophobia, the main reason for refusal of an MRI, and gadolinium-related risks or allergies are not concerns associated with PEM. In addition to patient refusal, it has been especially challenging to implement MRI in community settings partly due to the lack of recommended standard criteria for image acquisition and interpretation which has led to variable practice outcomes and therefore variable acceptance of the procedure by referring physicians [12]. While MRI has been successfully implemented in numerous medical communities as a valuable tool to diagnose ipsilateral cancer and detect unsuspected contralateral disease in 3–9% of patients, improving surgical management, these benefits are not without additional costs and consequences [43–46]. For instance, MRI equipment and installation costs are expensive, extensive time is required to train staff and physicians, and the technique has increased the number of unnecessary presurgical biopsy procedures. Disappointingly, studies suggest that only one of four MRI-guided biopsies finds cancer [47, 48]. Consequently, both referring surgeons and patients are frustrated with the high rate of FP findings and resultant patient anxiety.

A limitation of this study, as for many clinical trials, was disqualification of patients because of poor patient compliance. The patients were also not randomized for imaging, replicating clinical practice procedures in order to not compromise patient care and as for most single-site studies, the population was homogeneous. It is also important to emphasize that the study design did not address whether or how PEM image results alone influenced surgical treatment because all imaging results were made available to the surgeon prior to surgery. We must also emphasize that PEM technology is continually developing and physicians are gaining knowledge on how to utilize this technology effectively. The present study was conducted using a Solo I model of the Naviscan PEM scanner that does not have motorized paddles, like currently commercially available Solo II PEM scanners developed by Naviscan Inc.; hence, positioning patients by the technologist for imaging was difficult, resulting in 25% (3/12) FN index lesions. In order to overcome some of these limitations, the authors of this study are participating in a larger multi-site trial that includes diverse ethnicities and randomization of imaging modalities using the Solo II with motorized paddles.

PEM imaging can both identify worrisome breast lesions as well as provide an in vivo characterization of their glucose metabolism which in malignancies has been shown to correlate with high growth rates, aggressiveness, and capillary number [49]. An alternative molecular imaging approach is breast-specific gamma imaging (BSGI), which utilizes ^{99m}Tc-sestamibi. Direct comparison of PEM and BSGI is lacking and comparing prospective (PEM imaging) and retrospective studies (BSGI) is problematic. However, a study involving 23 subjects compared breast MRI to BSGI and found a malignancy specificity of 25% for MRI versus 71% for BSGI with equal sensitivity [50]. In another retrospective study with 146 subjects, BSGI had a higher 96.4% sensitivity at the expense of a lower specificity of 59.5% [51]. For comparison, the prospective study by Berg et al. [21] involving 94 subjects found PEM to have a 90% sensitivity with a specificity of 86%, suggesting comparable levels of both sensitivity and specificity within this subject cohort. This finding suggests imaging glucose metabolism may provide high sensitivity without a loss in specificity as is seen with other imaging approaches.

The most important result from this study is that PEM and breast MRI had the same overall sensitivity for depiction of index cancerous lesions including invasive cancer and DCIS. The trend of improved specificity of PEM for ipsilateral lesion detection warrants future investigation with a study that is powered to evaluate this outcome. Thus, PEM should be considered as an acceptable alternative to breast MRI as a presurgical managing option for many women who currently cannot tolerate a breast MRI, have scheduling constraints due to their hormonal status/menstrual cycle, and for use in communities struggling to implement a successful breast MRI program or those patients without access to breast MRI.

Acknowledgements We would like to thank Dr. Bhawanjit Brar for editorial and statistical review of this manuscript.

Conflicts of interest This study was supported solely by Boca Raton Regional Hospital. All data reside with the primary author, Kathy Schilling. WBPET and MRI were billed to the patients' insurance. All authors have no conflict of interest with the exception of Deepa Narayanan and Judith E. Kalinyak. Ms. Narayanan was previously employed by Naviscan Inc. and is a current stockholder. Ms. Narayanan assisted with the development of the clinical report

form used in this study, in data analysis and provided manuscript input and edits. Dr. Kalinyak is the Medical Director at Naviscan Inc. and assisted in study design, clinical report forms, and current manuscript input and edits. Dr. Kalinyak holds Naviscan stock options.

References

1. Elmore JG, Armstrong K, Lehman CD, Fletcher SW. Screening for breast cancer. JAMA 2005;293:1245–56.
2. Kalager M, Haldorsen T, Bretthauer M, Hoff G, Thoresen SO, Adami HO. Improved breast cancer survival following introduction of an organized mammography screening program among both screened and unscreened women: a population-based cohort study. Breast Cancer Res 2009;11:R44.
3. Tafra L. Positron emission mammography: a new breast imaging device. J Surg Oncol 2008;97:372–3.
4. Mushlin Al, Kouides RW, Shapiro DE. Estimating the accuracy of screening mammography: a meta-analysis. Am J. Pre Med 1998;14(2):143–53.
5. Tafra L, Fine R, Whitworth P, Berry M, Woods J, Ekbom G, et al. Prospective randomized study comparing cryo-assisted and needle-wire localization of ultrasound-visible breast tumors. Am J Surg 2006;192:462–70.
6. Enriquez L, Listinsky J. Role of MRI in breast cancer management. Cleve Clin J Med 2009;76(9):525–32.
7. Biglia N, Mariani L, Sgro L, Mininanni P, Moggio G, Sismondi P. Increased incidence of lobular breast cancer in women treated with hormone replacement therapy: implications for diagnosis, surgical and medical treatment. Endocr Relat Cancer 2007;14:549–67.
8. Degani H, Chetrit-Dadiani M, Bogin L, Furman-Haran E. Magnetic resonance imaging of tumor vasculature. Thromb Haemost 2003;89:25–33.
9. Furman-Haran E, Kelcz F, Degani H. Magnetic resonance imaging of breast cancer angiogenesis: a review. J Exp Clin Cancer Res 2002;21:47–54.
10. Kriege M, Brekelmans CT, Boetes C, Besnard PE, Zonderland HM, Obdeijn IM, et al. Efficacy of MRI and mammography for breast-cancer screening in women with a familial or genetic predisposition. N Engl J Med 2004;351:427–37.
11. Bassett LW, Dhaliwal SG, Eradat J, et al. National trends and practices in breast MRI. AJR Am J Roentgenol 2008;191(2):332–339.
12. Kuhl C. The current status of breast MR imaging. Part I. Choice of technique, image interpretation, diagnostic accuracy, and transfer to clinical practice. Radiology 2007;244:356–78.
13. Heywang-Köbrunner SH, Viehweg P, Heinig A, Küchler C. Contrast-enhanced MRI of the breast: accuracy, value, controversies, solutions. Eur J Radiol 1997;24:94–108.
14. Liberman L, Morris EA, Dershaw DD, Abramson AF, Tan LK. MR imaging of the ipsilateral breast in women with percutaneously proven breast cancer. AJR Am J Roentgenol 2003;180:901–10.
15. Grobner T. Gadolinium—a specific trigger for the development of nephrogenic fibrosing dermopathy and nephrogenic systemic fibrosis? Nephrol Dial Transplant 2006;21:1104–8.
16. Kribben A, Witzke O, Hillen U, Barkhausen J, Daul AE, Erbel R. Nephrogenic systemic fibrosis: pathogenesis, diagnosis, and therapy. J Am Coll Cardiol 2009;53:1621–8.
17. Weinberg I, Beylin D, Zavarzin V, Yarnall S, Stepanov PY, Anashkin E, et al. Positron emission mammography: high-resolution biochemical breast imaging. Technol Cancer Res Treat 2005;4:55–60.
18. Weinberg IN. Applications for positron emission mammography. Phys Med 2006;21:132–7.
19. Weinberg I, Beylin D, Yarnall S, Anashkin E, Stepanov P, Dolinsky S, et al. Applications of a PET device with 1.5 mm FWHM intrinsic spatial resolution to breast cancer imaging. Proceedings of the 2004 IEEE International Symposium on Biomedical Imaging: From Nano to Macro, Arlington, VA, 2004, New York: IEEE, 2004; 1396–99.
20. Avril N, Adler LP. F-18 fluorodeoxyglucose-positron emission tomography imaging for primary breast cancer and loco-regional staging. Radiol Clin North Am 2007;45:645–57.
21. Berg WA, Weinberg IN, Narayanan D, Lobrano ME, Ross E, Amodei L, et al. High-resolution fluorodeoxyglucose positron emission tomography with compression ("positron emission mammography") is highly accurate in depicting primary breast cancer. Breast J 2006;12:309–23.
22. Berg WA, Madsen KS, Schilling K, Tartar M, Pisano ED, Hovanessian Larsen L, et al. Comparative Effectiveness of Positron Emission Mammography and MRI for Presurgical Planning of the Ipsilateral Breast in Women with Breast Cancer. Radiology 2010; in press.
23. Ikeda DM, Hylton NM, Kuhl CK, et al. Breast Imaging Reporting and Data System, BI-RADS: Magnetic Resonance Imaging. Reston: American College of Radiology; 2003.
24. Narayanan D, Kalinyak JE, Berg WA. Interpretation of Positron Emission Mammography (PEM) by Experienced Breast Imaging Radiologists: Comparison to MRI. AJR Am J Roentgenol 2010; in press.
25. Narayanan D, Madsen KS, Kalinyak JE, Berg WA. Interpretation of Positron Emission Mammography: Feature Analysis and Rates of Malignancy. AJR Am J Roentgenol 2010; in press.
26. Santra A, Kumar R, Reddy R, Halanaik D, Kumar R, Bal CS, et al. FDG PET-CT in the management of primary breast lymphoma. Clin Nucl Med 2009;34:848–53.
27. Ueda S, Tsuda H, Asakawa H, Shigekawa T, Fukatsu K, Kondo N, et al. Clinicopathological and prognostic relevance of uptake level using 18F-fluorodeoxyglucose positron emission tomography/computed tomography fusion imaging (18F-FDG PET/CT) in primary breast cancer. Jpn J Clin Oncol 2008;38:250–8.
28. Jemal A, Siegel R, Ward E, Hao Y, Xu J, Thun MJ. Cancer statistics, 2009. CA Cancer J Clin 2009;59:225–49.
29. Levine EA, Freimanis RI, Perrier ND, Morton K, Lesko NM, Bergman S, et al. Positron emission mammography: initial clinical results. Ann Surg Oncol 2003;10:86–91.
30. Rosen EL, Turkington TG, Soo MS, Baker JA, Coleman RE. Detection of primary breast carcinoma with a dedicated, large-field-of-view FDG PET mammography device: initial experience. Radiology 2005;234:527–34.
31. Tafra L, Cheng Z, Uddo J, Lobrano MB, Stein W, Berg WA, et al. Pilot clinical trial of 18F-fluorodeoxyglucose positron-emission mammography in the surgical management of breast cancer. Am J Surg 2005;190:628–32.
32. Berg WA, Gutierrez L, NessAiver MS, Carter WB, Bhargavan M, Lewis RS, et al. Diagnostic accuracy of mammography, clinical examination, US, and MR imaging in preoperative assessment of breast cancer. Radiology 2004;233:830–49.
33. Vranjesevic D, Schiepers C, Silverman DH, Quon A, Villalpando J, Dahlborn M, et al. Relationship between 18F-FDG uptake and

breast density in women with normal breast tissue. J Nucl Med 2003;44:1238–42.
34. Kumar R, Mitchell S, Alavi A. 18F-FDG uptake and breast density in women with normal breast tissue. J Nucl Med 2004;45:1423.
35. Delille JP, Slanetz PJ, Yeh ED, Kopans DB, Garrido L. Physiologic changes in breast magnetic resonance imaging during the menstrual cycle: perfusion imaging, signal enhancement, and influence of the T1 relaxation time of the breast tissue. Breast J 2005;11:236–41.
36. Mavi A, Cermik TF, Urhan M, Puskulcu H, Basu S, Cucchiara AJ, et al. The effect of age, menopausal state, and breast density on (18)F-FDG uptake in normal glandular breast tissue. J Nucl Med 2010;51:347–52.
37. Wahl RL. Current status of PET in breast cancer imaging, staging, and therapy. Semin Roentgenol 2001;36:250–60.
38. Avril N, Rosé CA, Schelling M, Dose J, Kühn W, Bense S, et al. Breast imaging with positron emission tomography and fluorine-18 fluorodeoxyglucose: use and limitations. J Clin Oncol 2000;18:3495–502.
39. Mavi A, Urhan M, Yu JQ, Zhuang H, Houseni M, Cermik TF, et al. Dual time point 18F-FDG PET imaging detects breast cancer with high sensitivity and correlates well with histologic subtypes. J Nucl Med 2006;47:1440–6.
40. Zytoon AA, Murakami K, El-Kholy MR, El-Shorbagy E. Dual time point FDG-PET/CT imaging. Potential tool for diagnosis of breast cancer. Clin Radiol 2008;63:1213–27.
41. Mankoff DA, Dunnwald LK, Kinahan P. Are we ready for dedicated breast imaging approaches? J Nucl Med 2003;44:594–5.
42. Berg WA, Blume JD, Adams AM, Jong RA, Barr RG, Lehrer DE, et al. Reasons women at elevated risk of breast cancer refuse breast MR imaging screening: ACRIN 6666. Radiology 2010;254:79–87.
43. Lee SG, Orel SG, Woo IJ, Cruz-Jove E, Putt ME, Solin LJ, et al. MR imaging screening of the contralateral breast in patients with newly diagnosed breast cancer: preliminary results. Radiology 2003;226:773–8.
44. Lehman CD, Blume JD, Thickman D, Bluemke DA, Pisano E, Kuhl C, et al. Added cancer yield of MRI in screening the contralateral breast of women recently diagnosed with breast cancer: results from the International Breast Magnetic Resonance Consortium (IBMC) trial. J Surg Oncol 2005;92:9–15.
45. Lehman CD, Gatsonis C, Kuhl CK, Hendrick RE, Pisano ED, Hanna L, et al. MRI evaluation of the contralateral breast in women with recently diagnosed breast cancer. N Engl J Med 2007;356:1295–303.
46. Liberman L, Morris EA, Kim CM, Kaplan JB, Abramson AF, Menell JH, et al. MR imaging findings in the contralateral breast of women with recently diagnosed breast cancer. AJR Am J Roentgenol 2003;180:333–41.
47. Han BK, Schnall MD, Orel SG, Rosen M. Outcome of MRI-guided breast biopsy. AJR Am J Roentgenol 2008;191:1798–809.
48. Schell AM, Rosenkranz K, Lewis PJ. Role of breast MRI in the preoperative evaluation of patients with newly diagnosed breast cancer. AJR Am J Roentgenol 2009;192:1438–44.
49. Raylman RR, Majewski S, Smith MF, Proffitt J, Hammond W, Srinivasan A, et al. The positron emission mammography/tomography breast imaging and biopsy system (PEM/PET): design, construction and phantom-based measurements. Phys Med Biol 2008;53:637–53.
50. Brem RF, Petrovitch I, Rapelyea JA, Young H, Teal C, Kelly T. Breast-specific gamma imaging with 99mTc-sestamibi and magnetic resonance imaging in the diagnosis of breast cancer—a comparative study. Breast J 2007;13:465–9.
51. Brem RF, Floerke AC, Rapelyea JA, Teal C, Kelly T, Mathur V. Breast-specific gamma imaging as an adjunct imaging modality for the diagnosis of breast cancer. Radiology 2008;247(3):651–7.